Improvement of the temporal contrast of a femtosecond laser pulse with a non-linear Sagnac interferometer

Laboratoire d'Optique Appliquée
ENSTA, École Polytechnique, CNRS

Master Thesis
by
Matilda Träff

Lund Reports on Atomic Physics, LRAP -269
Lund, March 2001

Abstract

A new method to improve the temporal contrast of an ultra short intense pulse has been developed at the Laboratoire d'Optique Appliquée, in Paris. The technique uses a Sagnac interferometer in combination with a non-linear element. An introduced phase shift in the ultra short pulse separates it from the background, consisting of amplified spontaneous emission. The theoretical results showed a possible improvement of the contrast of more than four orders of magnitude. An extinction of the fluorescence from a 1 kHz, 50 fs laser, of four orders of magnitude was obtained, in accordance with the theory. Experiments with femtosecond pulses were also performed.

Contents

1 Introduction

1.1 History

In our universe, the laser is not a new phenomenon. Natural lasers, and masers, are oscillating in interstellar clouds, comets and in the atmospheres of Venus and Mars, and they have probably been doing this for eons [1]. However, the appearance of lasers on Earth is quite recent. It was not until 1917 that Einstein gave a quantum mechanical treatment of stimulated emission of radiation, which is the basic idea of all lasers (the word laser is an acronym for *"Light Amplification by Stimulated Emission of Radiation"*). The first practical realization of these discoveries was then not performed until 1954, when C. H. Townes, assisted by J. P. Gordon and H. Zeiger, succeeded in constructing a functional ammonia maser (an acronym obtained from the preceding one, with light substituted for microwave) [2]. For this, they received the Nobel Prize ten years later.

The first real laser was constructed in 1960, by Theodore H. Maiman [3]. It was a ruby laser with a central wavelength of 6943 Å, operating in free running mode. During the last forty years, discoveries such as Q-switching, mode locking and chirped pulse amplification (CPA) have led to increasing power and decreasing pulse duration for the lasers. Figure 1.1 shows the evolution of these two laser characteristics during the last four decades, in broad outline. The stagnation of the power for about twenty years was due to difficulties concerning non-linear optics, which was solved by the CPA technique. A pulse duration of six femtoseconds was obtained as early as 1987, with a dye laser combined with an optical fiber [4]. The more recent solid state lasers can not yet perform much better than that, due to the time-bandwidth limitation[1]. A pulse duration of less than five femtoseconds have, however, been performed with a solid state laser [5]. The great advantage, compared to the earlier lasers, is that the short time duration is achieved with a small, easy to handle-laser. Also, the solid state lasers are much more powerful than the earlier ones, and they have accordingly made new domains of research accessible.

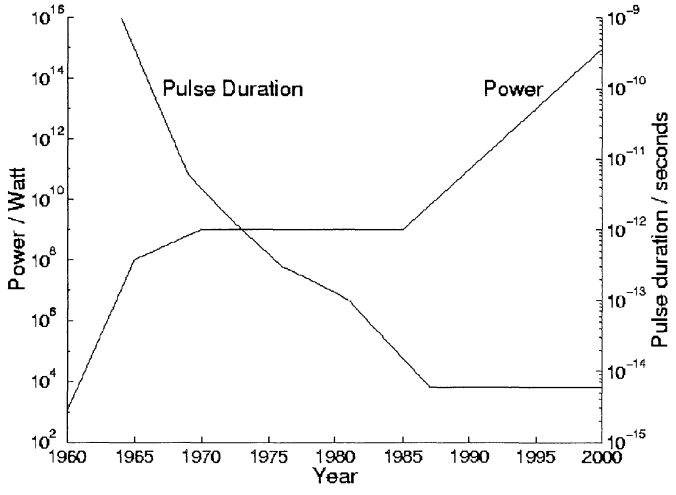

Figure 1.1 Power and pulse duration for lasers as a function of years. Data for the power and pulse duration curves was found in [6] and [7], respectively.

[1] $\tau \times \Delta\nu \geq$ constant

1.2 The Femtosecond Pulses in Brief

It is hard to imagine a time as short as one femtosecond. It may be helpful to know that a femtosecond is to a second what 0,1 mm is to the distance between the Earth and the sun, or that when light travels about the distance from here to the moon in one second, it travels 0,3 μm in one femtosecond. That is about half the wavelength of red light.

With laser pulses of this time duration new fields in science become accessible. For example one can, by hitting a solid target with a femtosecond pulse, create a plasma. This leads to emission of hard x-rays and fast electron x-rays. Experiments are also performed with gas targets. This interaction can result in acceleration of electrons, coherent x-ray lasers and hard x-rays. The above mentioned experiments are currently being worked on at the Laboratoire d'Optique Appliquée in Paris, and in many other laboratories. Similarly, in other fields of science, the femtosecond pulses have turned out to be an important source for successful experiments. One example is in chemistry, where very fast events can be observed.

However, in numerous experiments, especially those performed with solid targets, it is hard to obtain satisfying results because of the amplified spontaneous emission, ASE. It creates a background of light out of phase with the laser beam. The peak intensity divided by the intensity of the ASE, is called contrast. With the high energies needed for the above mentioned experiments, the ASE contains enough energy to turn the solid into plasma before the main pulse arrives, see Figure 1.2. Naturally, this makes interpretation of the results difficult, or even impossible.

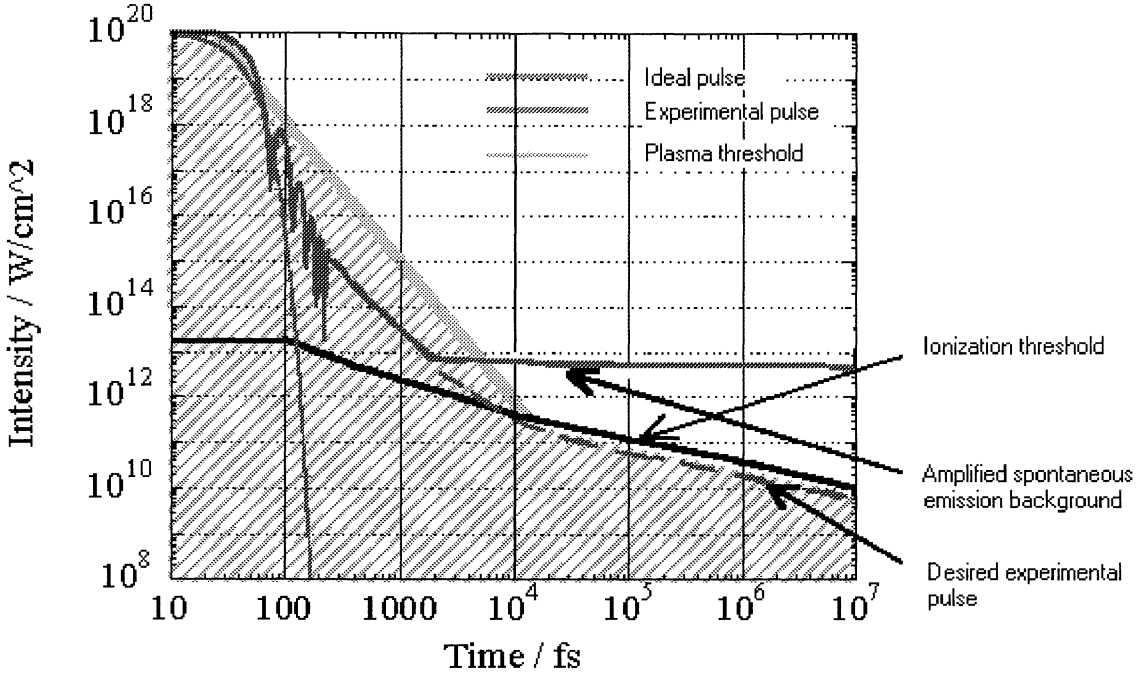

Figure 1.2 Schematic description of a femtosecond pulse with respect to different regimes of interaction. The ideal pulse is Gaussian, and the experimental curve is an estimation of a real femtosecond pulse. The long pulse background is the ASE. The lower solid line shows the intensity where the solid is ionized. If the plasma threshold is passed, the solid will turn into plasma. To obtain a satisfying result the beam should, as indicated by the broken line, lie in the region to the left of the plasma threshold, and below the ionization threshold. This is obviously impossible if the contrast is not improved.

1.3 The Purpose of This Master Thesis

This master thesis was carried out at Laboratoire d'Optique Appliquée (LOA) in Paris, France. LOA is under the authority of École Nationale Supérieure de Techniques Avancées (ENSTA), École Polytechnique and Centre National de la Recherche Scientifique (CNRS).

The purpose of this master thesis was to increase the temporal contrast of a femtosecond pulsed laser. This was to be done with a Sagnac interferometer combined with non-linear optics. The first task was to investigate different possible ways to realize this, by collecting material and by making simulations in Matlab. The second part consisted in verifying if the theory agreed with reality, by putting together the experimental setup and performing experiments.

Because this is a new technique with a lot of interest worldwide, the subject of this thesis has been accepted for oral presentation at the Conference on Lasers and Electro-Optics (CLEO) in Baltimore, USA, in may 2001. The work will also be published in a scientific journal.

2 The Laser Chain

The prospective aim of this master thesis is to implement the non-linear Sagnac interferometer in the laser chain in Salle Jaune at LOA, to improve the contrast of this laser, see Figure 2.1.

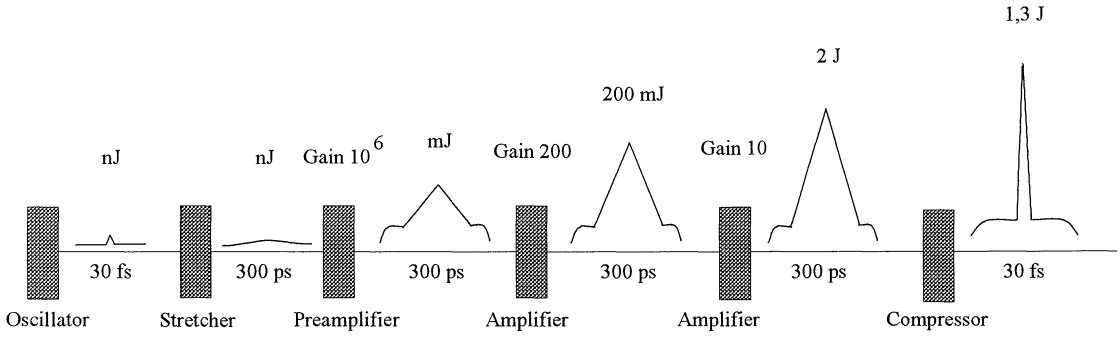

Figure 2.1 An overview of the pulse at different stages in the laser chain in Salle Jaune at LOA in Paris. The "feet" of the pulse is due to ASE.

The oscillator is the source of the laser pulse. It creates a beam with low energy (nJ) and high repetition rate (MHz). In the stretcher the beam is extended in time, to support a high amplification without damaging the optical components. A Pockels cell then selects the repetition rate of the pulse to be amplified, in this case 10 Hz. After the preamplifier, the beam energy is in the order of mJ, and a significant amount of ASE has been introduced. In the following amplification processes the gain is considerably lower, and the ASE is much less disturbing. In the compressor, finally, the beam is ideally recompressed to its initial time duration. Some of the energy is lost during this process, because of losses in the gratings. The amplification process is referred to as chirped pulse amplification, and is a widely used method in ultra short laser chains nowadays. More information about this method and the different parts of the chain is found in [8].

The Sagnac interferometer is to be placed after the preamplifier. Since it works with femtosecond pulses, it will be put between an additional compressor and stretcher. If a good contrast can be obtained at this part of the chain, it will be kept fairly well during the final stages, since the main amplification is already effected. For a more detailed view of the laser chain, see Figure 2.2.

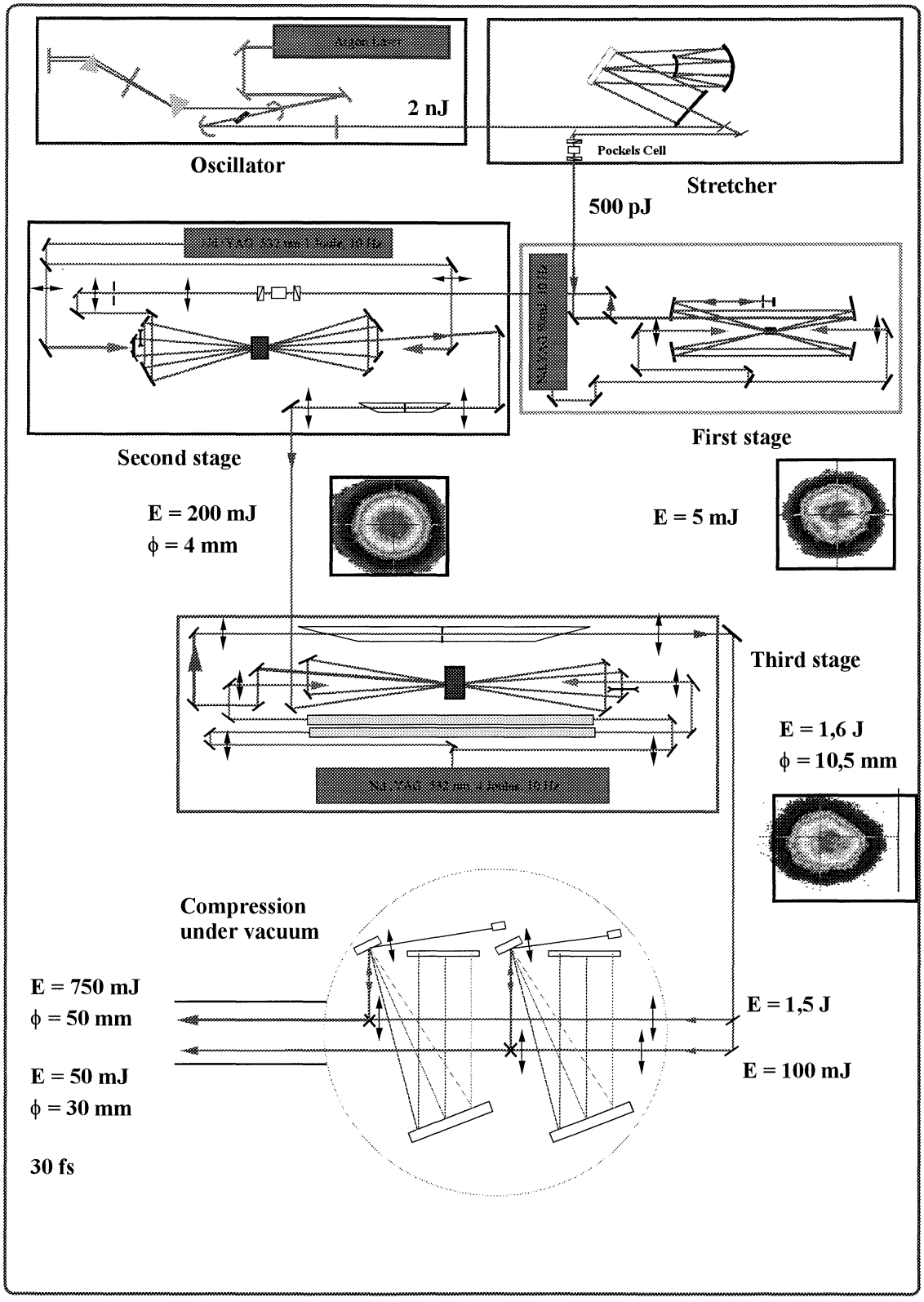

Figure 2.2 Detailed view of the laser chain in Salle Jaune at LOA in Paris.

3 Theory

3.1 Contrast Theory

3.1.1 Amplified Spontaneous Emission (ASE)

In a laser system the activated media in the oscillator and in the amplifiers emit photons spontaneously, in all directions. The first photon emitted along the cavity axis in the oscillator gives rise to the stimulated emission that is the basis of the laser. Most of the spontaneously emitted photons do not affect the laser beam since their directions are not within the solid angle Ω of the beam, and the received amplification is insignificant, see Figure 3.1. Naturally, some of these photons are emitted close to the solid angle, but will still not disturb the beam, since they are lost during the further amplification process. However, those photons spontaneously emitted within the solid angle, will be amplified and cause an undesirable background of the laser beam. This part of the beam is referred to as amplified spontaneous emission, or ASE.

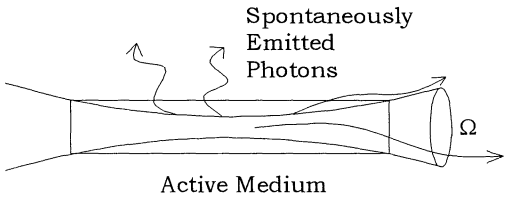

Figure 3.1 Schematic view of an active medium with solid angle Ω.

The ASE possesses some characteristics that are similar to those of laser light:

- Its propagation mode is equal to the one of the laser beam.
- In our case, the spectral bandwidth of the ASE is of the same order of magnitude as for the femtosecond pulse, that is about 30 nm.
- If the pumping is strong enough to raise a very large fraction of atoms to the upper level in the active medium, the ASE can contain a significant amount of the beam's energy. After the first step in the amplification process, the energy of the ASE counts a few percent of the total beam energy. Further on, in steps two and three, the fraction of energy originating from ASE will rise, and can in the worst cases reach a level of fifty percent in the end.

The one significant difference between laser light and ASE is that the laser light is coherent whereas the ASE shows no spectral coherence, i.e. the different wavelengths of the beam have no phase relation. The ASE thus creates a background of light that is out of phase with the light of the laser, and provided it is possible, we wish to avoid amplification of this background, which in most of the cases is undesirable.

3.1.2 Temporal Contrast

One of the basic requirements for a laser system is that the stimulated emission greatly exceeds the spontaneous emission in intensity. However, as mentioned above, sometimes the ASE can reach such a level that it is no longer negligible.

A measure of the relation between the peak intensity and the background intensity is called Intensity Contrast Ratio (ICR) or "contrast". For a 780 nm Ti:sapphire femtosecond laser the ICR is typically of the order of 10^6, after passage through the entire laser chain. The focused intensity of such a laser can reach a level of 10^{19} W/cm^2, and accordingly the ASE intensity can be as high as 10^{13} W/cm^2 [9]. This is far above the ionization threshold for several materials (according to Figure 1.2) and consequently when the main pulse arrives it will be focused, not on the solid one intended to study, but on a plasma. Clearly, a low ICR can make interesting and essential experiments impossible, and it is therefore of the outmost importance to improve the contrast.

At the output of the oscillator of the femtosecond laser in Salle Jaune at LOA, there is almost no ASE present. Measures have been made with a third order correlator, showing a contrast of 10^9 of the beam, see Figure 3.2.

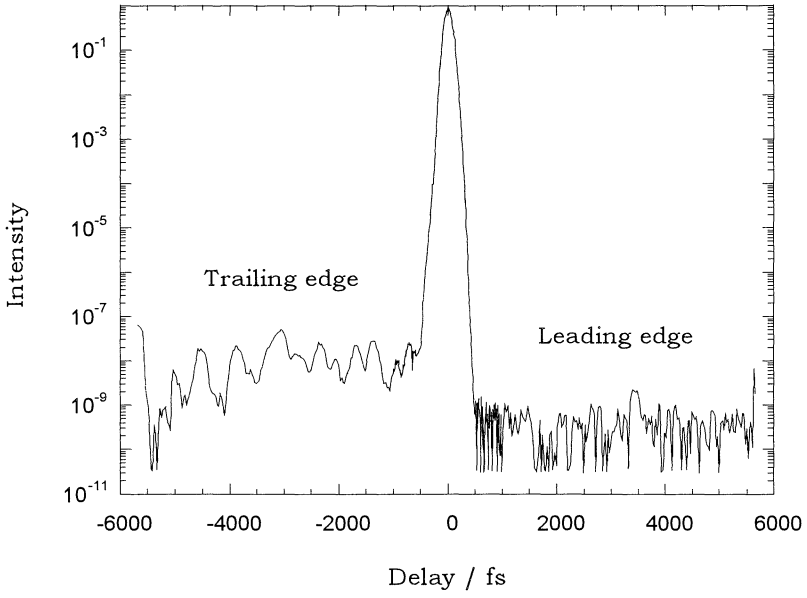

Figure 3.2 The contrast of the beam at the output of a Kerr lens mode locked Ti:sa oscillator, similar to the one in Salle Jaune at LOA.

Instead, it is the ASE arising from the active medium in the first amplifier of the chain, that is our concern. The reason is that, at this point in the amplification process, the gain is extremely high. It reaches a level of six to seven orders of magnitude. In the following two amplifiers, the gain is only about two and one orders of magnitude, respectively.

Experiments have been made and published [10], showing an improvement of the contrast of two orders of magnitude with the use of a saturable absorber. This is not enough, and our wish was to go further and reach an amelioration of the contrast of three or four orders of magnitude. To do this we used a Sagnac interferometer in combination with non-linear optics, inserted behind the first amplifier of the chain.

3.2 The Linear Sagnac Interferometer

Mr Georges Sagnac [11] was born in Périgueux, France, in 1869, into a bourgeois family. At the age of twenty, he began his studies at École Normale Supérieure in Paris. At thirty-one he became professor of physics at the University of Lille, after being awarded the *docteur ès sciences* degree. About ten years later he received a professor of physics title at the University of Paris as well. Twice he was nominated for the physics section of the Academy, but he was never elected.

His major interests were optics of interference and radiation produced by x-rays. From the age of forty he was primarily engaged in the design of an interferometer, the Sagnac interferometer, thanks to which he is well remembered today. During his life, he was a staunch classicist, and he interpreted all his results as contradicting Einstein's theory of relativity. He died in 1928, fifty-eight years old.

3.2.1 The Functioning of the Linear Sagnac Interferometer

The Sagnac interferometer is illustrated in Figure 3.3 below. The beam enters at point A with an angle of incidence of 45°. At the reflecting surface of the beam splitter part of the beam is reflected, following path 1, and part of it is transmitted, following path 2. As the second surface of the beam splitter is treated with an anti reflection coating, the two beams interfere at the reflecting surface, after having completed one turn in the interferometer each.

What is special about the Sagnac interferometer is that both beams travel along the same path and thus there is no phase shift introduced between the beams. It is therefore only the intensity of the entering beam and the reflectivity of the beam splitter that determine the intensity of the light leaving the interferometer (i.e. is not reflected back to the input A).

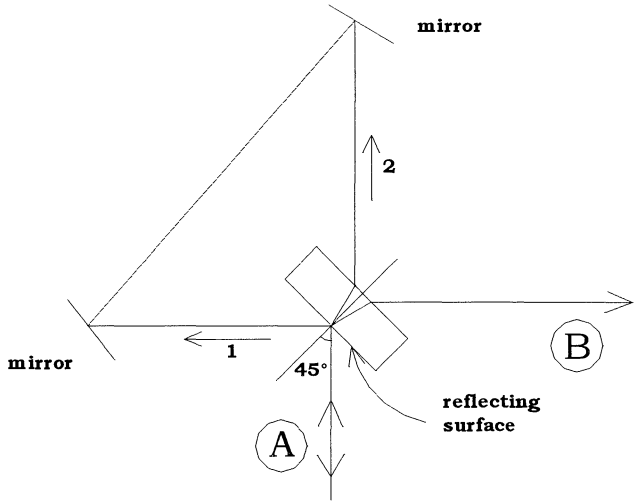

Figure 3.3 Schematic view of the linear Sagnac interferometer.

3.2.2 The Linear Sagnac Interferometer in Equations

We investigate more precisely what happens in the interferometer by deriving the equations stated below. In the calculations the following notations are used: The reflection and transmission coefficients of the beam splitter are denoted r and t, respectively. Further, the reflectivity $\Re$, and the transmission $\Im$, are obtained by raising these coefficients to the second power, i.e. $\Re = |r|^2$ and $\Im = |t|^2$. Naturally, for any material without absorption, $\Re + \Im$ equals one.

In Equations (3.1) and (3.2) the first term is originating from the part of the beam following path 1, and the second from the part following path 2, according to Figure 3.3. Thus, the amplitude coming back to point A, S_A, becomes:

$$S_A = A(r \times t + r \times t) = 2Art \tag{3.1}$$

where A is the incident beam's amplitude. And at point B the amplitude, S_B, becomes[2]:

$$S_B = A(r \times r \times e^{i\pi} + t \times t) = A(-r^2 + t^2) = A(\Im - \Re) \tag{3.2}$$

The intensities for the two directions are then, as $I = A^2$:

$$I_A = S_A \times S_A^* = 4A^2 r^2 t^2 = 4I\Re\Im \tag{3.3}$$

$$I_B = S_B \times S_B^* = I(\Im - \Re)^2 \tag{3.4}$$

By adding these intensities, the sum should, if we assume no losses in the mirrors or in the beam splitter, equal the incoming intensity I.

$$I_A + I_B = I(4\Re\Im + \Im^2 + \Re^2 - 2\Re\Im) = I(\Re + \Im)^2 \tag{3.5}$$

Since $\Re + \Im$ by definition is unity, we see that the sum of the intensities is I, just as expected.

Now, if $\Re = \Im = ½$ we note that the intensities become:

$I_A = I$

$I_B = 0$

---

[2] The factor $e^{i\pi}$ is due to the fact that the beam is reflected towards a lower index medium, in this case from glass towards air.

Consequently, by using a beam splitter with these properties, all the intensity entering the interferometer will return in the direction A. However, this is an ideal case, because $\mathfrak{R}$ and $\mathfrak{T}$ will never be exactly the same. As one can observe above in Equation (3.4), I_B is very sensitive to the difference between $\mathfrak{R}$ and $\mathfrak{T}$ and it is therefore of great importance to minimize this difference if no light is supposed to leave the interferometer.

Note that if the beam splitter is turned 180°, i.e. with the anti reflection coating on the opposite side, the equations will end up the same.

3.3 The Non-Linear Sagnac Interferometer

The non-linear Sagnac interferometer uses a non-linear element in combination with a neutral density, to obtain a phase shift between the two beams propagating in the interferometer.

3.3.1 Non-Linear Effects on a Propagating Beam

In most optical materials the refractive index, n, depends on the intensity I, at high intensities. That is:

$$n = n(I) \tag{3.6}$$

In a first order approximation this equation can be written:

$$n = n_0 + \delta n = n_0 + n_2 I \tag{3.7}$$

where n_0 is the linear index, n_2 is the non-linear index and I is the beam intensity. n_2 is commonly a positive constant of order 10^{-16} cm^2/W. The change in the optical refractive index produced by the beam itself is referred to as the optical Kerr effect.

A light beam propagating through a medium along the z-axis can be described with the following equation:

$$\psi = A_0 e^{i\varphi} = A_0 e^{i(kz-\omega t)} \tag{3.8}$$

where A_0 is the original amplitude and φ is the phase of the beam. k is the wave number and ω is the frequency of the light. The space dependent part of the phase is thus:

$$\varphi = kz = \frac{2\pi n}{\lambda} z \tag{3.9}$$

where n is the refractive index and λ is the wavelength of the light. A beam with intensity I that has propagated a distance L through a non-linear medium will obtain a phase difference equal to:

$$\varphi = \frac{2\pi L}{\lambda}(n_0 + n_2 I) \tag{3.10}$$

If two beams with different intensities propagate through the same non-linear medium, there will be a phase shift between them:

$$\delta\varphi = \frac{2\pi L n_2}{\lambda}\delta I \tag{3.11}$$

3.3.2 The Functioning of the Non-Linear Sagnac Interferometer

With the linear Sagnac interferometer there will be no improvement of the contrast since both the high intensity and the lower intensity ASE leave the interferometer in the same direction. By introducing a non-linear element in the beam path there will be a phase delay of the beam, due to the optical Kerr effect, which is dependent on the intensity. A neutral density τ (Figure 3.4) inserted in the path way decreases the intensity of beam 1 before arriving to the non-linear medium. As beam 2 propagates without obstacles to the non-linear medium, the intensity remains high and a phase difference $\Delta\varphi$ between the beams will arise. The fact that the intensity of beam 2 is decreased after the phase delay has been introduced has no influence on the difference of phase between the beams. It only affects the intensity of the exiting beam.

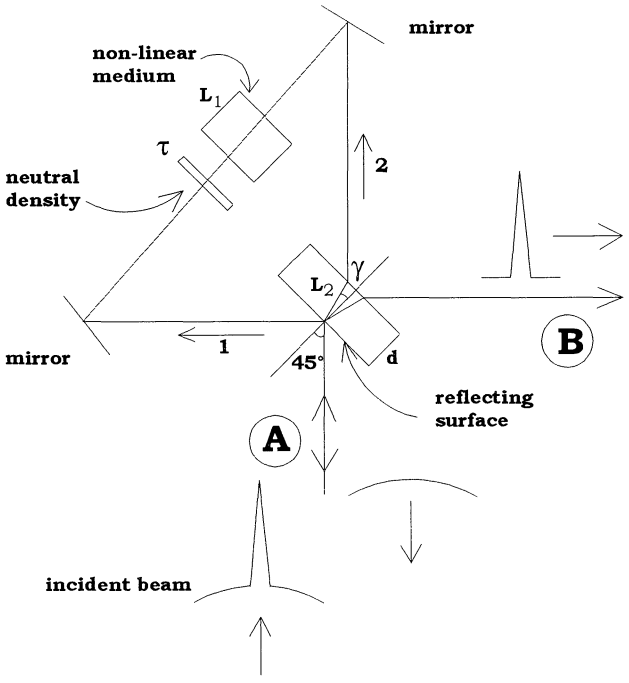

Figure 3.4 Schematic view of the non-linear Sagnac interferometer.

By arranging the different parameters it is now possible to obtain for example $\Delta\varphi = \pi$ for the high intensity light, which means that it will fully exit the interferometer in the direction B. The lower intensity ASE will experience a different phase shift, and ideally it will be entirely reflected back in the direction A. The ASE is thus separated from the ultra intense pulse, and the contrast is improved, as illustrated in Figure 3.4. In the next section these relations are analyzed in more detail.

3.3.3 The Non-Linear Sagnac Interferometer in Equations

To derive the phase difference in the direction B, the expression for the amplitude in the same direction is first considered. S_1 corresponds to the beam following path 1 and S_2 to the beam following path 2, according to Figure 3.4. A is the incident amplitude whereas r and t are the reflection and transmission coefficients of the beam splitter, respectively. The reflectivity and transmission are denoted $\Re$ and $\Im$. $I = A^2$.

$$S_1 = A(r \times \tau \times e^{i\alpha\tau^2\Re I} \times e^{i\beta\tau^2\Re I} \times e^{i\pi} \times r \times e^{i\beta\tau^2\Re^2 I}) = -A\Re\tau \times e^{i(\alpha+\beta)\tau^2\Re I} \times e^{i\beta\tau^2\Re^2 I} \tag{3.12}$$

where $\alpha = 2\pi n_2 L_1 / \lambda$ and $\beta = 2\pi n_2 L_2 / \lambda$

$$S_2 = A(t \times e^{i\beta\Im I} \times e^{i\alpha\Im I} \times \tau \times t \times e^{i\beta\tau^2\Im^2 I}) = A\Im\tau \times e^{i(\alpha+\beta)\Im I} \times e^{i\beta\tau^2\Im^2 I} \tag{3.13}$$

This gives the total amplitude at B:

$$S_{total} = S_1 + S_2 = A\tau(-\Re e^{i(\alpha+\beta)\tau^2\Re I} \times e^{i\beta\tau^2\Re^2 I} + \Im e^{i(\alpha+\beta)\Im I} \times e^{i\beta\tau^2\Im^2 I}) \tag{3.14}$$

Suppose that $\Re = \Im = ½$. S_{total} then becomes:

$$S_{total} = A\frac{\tau}{2} \times (-e^{i(\alpha+\beta)\tau^2\frac{I}{2}} \times e^{i\beta\tau^2\frac{I}{4}} + e^{i(\alpha+\beta)\frac{I}{2}} \times e^{i\beta\tau^2\frac{I}{4}}) =$$

$$= A\frac{\tau}{2} \times e^{i\beta\tau^2\frac{I}{4}}(e^{i(\alpha+\beta)\frac{I}{2}} - e^{i(\alpha+\beta)\tau^2\frac{I}{2}}) \tag{3.15}$$

The intensity in the direction B can then be written:

$$I_B = S_{total} \times S^*_{total} = A^2\frac{\tau^2}{4} \times e^{i\beta\tau^2\frac{I}{4}}(e^{i(\alpha+\beta)\frac{I}{2}} - e^{i(\alpha+\beta)\tau^2\frac{I}{2}}) \times e^{-i\beta\tau^2\frac{I}{4}}(e^{-i(\alpha+\beta)\frac{I}{2}} - e^{-i(\alpha+\beta)\tau^2\frac{I}{2}}) =$$

$$= I\frac{\tau^2}{4} \times (e^{i(\alpha+\beta)\frac{I}{2}} - e^{i(\alpha+\beta)\tau^2\frac{I}{2}}) \times (e^{-i(\alpha+\beta)\frac{I}{2}} - e^{-i(\alpha+\beta)\tau^2\frac{I}{2}}) =$$

$$= I\frac{\tau^2}{4} \times (1+1-e^{i(\alpha+\beta)(1-\tau^2)\frac{I}{2}} - e^{-i(\alpha+\beta)(1-\tau^2)\frac{I}{2}}) =$$

$$= I\frac{\tau^2}{2} \times (1 - \cos\Delta\varphi) \tag{3.16}$$

where $\Delta\varphi = \frac{(\alpha + \beta)}{2}(1 - \tau^2)I$ (3.17)

Note that for $\tau = 1$, which means that no difference in intensity between beam 1 and 2 is introduced, $\Delta\varphi$ equals zero and consequently no light leaves the interferometer. To maximize I_B the phase shift has to be π (or $\pi + 2\pi n$ where n is an integer). Under these conditions I_B equals the incoming intensity (I) times τ^2.

3.3.4 Numerical Estimation of Appropriate Beam Size

For all notations, see Figure 3.4. The following values are assumed:

$n_{air} = 1{,}0$

$n_{glass} = 1{,}46$ (fused silica)

$n_2 = 3{,}2 \times 10^{-16}$ cm²/W (fused silica)

$L_1 = 2{,}0$ cm

$d = 0{,}50$ cm

$\gamma = \arcsin((\frac{n_{air}}{n_{glass}}) \sin 45°) = 29{,}0°$

$L_2 = \frac{d}{\cos\gamma} = 0{,}57$ cm

$\tau = 0{,}40$

$\lambda = 0{,}80 \times 10^{-4}$ cm

These values give:

$\alpha = 2\pi n_2 L_1 / \lambda = 1{,}6\pi 10^{-11}$ cm²/W and

$\beta = 2\pi n_2 L_2 / \lambda = 4{,}6\pi 10^{-12}$ cm²/W

This gives the phase difference:

$$\Delta\varphi = \frac{(\alpha + \beta)}{2}(1 - \tau^2)I = 8{,}6\pi 10^{-12} I$$

To attain a phase difference of π, I needs to be:

$$I = \frac{1}{8{,}6 \times 10^{-12}} = 1{,}20 \times 10^{11} \text{ W/cm}^2$$

Further it is assumed that the laser possesses the following characteristics:

$E = 1{,}0$ mJ

$\Delta t = 30$ fs

The power per pulse is then:

$$P = \frac{E}{\Delta t} = \frac{10^{-3}}{30 \times 10^{-15}} = 3{,}30 \times 10^{10} \text{ W}$$

Since P equals the beam intensity times its cross section area, I is:

$$I = \frac{2P}{\pi w^2} = \frac{6{,}7 \times 10^{10}}{\pi w^2}$$

where w is the beam radius (see Appendix A), and the factor 2 is due to the fact that the pulse is Gaussian.

By using the above calculated I, the corresponding radius becomes:

$w = 0{,}42 \text{ cm} = 4{,}2 \text{ mm}$

And so the beam diameter is:

$D = 8{,}4 \text{ mm}$

By adjusting the size of the laser beam, the intensity can be controlled. This is achieved by putting a so called telescope in the beam path. A large beam gives a lower intensity and vice versa. With the above calculated beam size it should be possible to obtain the intensity that gives the wanted phase shift.

3.4 Spectral Effects

The first task was to perform simulations in Matlab, in order to find an appropriate beam splitter for the interferometer. As mentioned before, the beam incident on the interferometer carries a background of ASE. As the intensity of the ASE is sufficiently low not to create non-linear effects, in the ideal case it will be completely reflected back to the input of the interferometer. It turns out, however, that the condition for this to happen, $\Re = \Im = 1/2$, is impossible to fulfil over the whole spectral range of the beam. Consequently, part of the ASE will leave the interferometer copropagating with the high intensity light.

Recall that at the output of the linear Sagnac interferometer the intensity is:

$$I_B = I(\Im - \Re)^2$$

where I_B is the amount of ASE leaving the interferometer.

To improve the contrast by a factor 10^6, $(\Im - \Re)^2$ needs to be 10^{-6}, or $(\Im - \Re)$ has to be 10^{-3}. An important task is thus to investigate how close to this condition we possibly can get over a wide spectral range. Under the optimal circumstances, an estimation of the fraction of the linear wave that leaves the interferometer will be performed, showing if our goal is in reach.

3.4.1 Beam Splitter based on FTIR

The first proposition was to use a beam splitter, consisting basically of two prisms with a thin layer of air in between, see Figure 3.5. By changing the distance between the prisms, and the incident angle of the light, the transmission can be brought as close to $\Im = 1/2$ as possible. The idea behind this beam splitter is a phenomenon referred to as frustrated total internal reflection, FTIR.

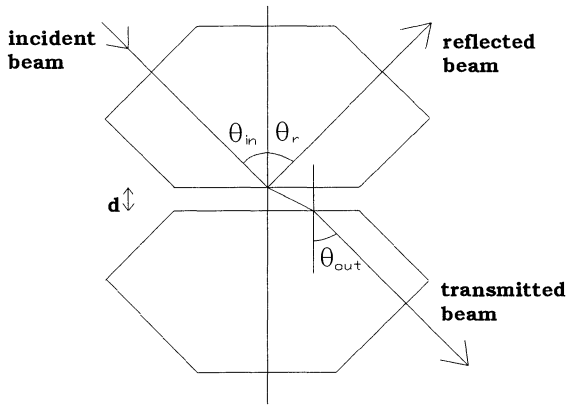

Figure 3.5 Schematic diagram of the FTIR beam splitter. $\theta_{in} = \theta_r = \theta_{out}$.

The physical phenomenon of frustrated total internal reflection is explained in Appendix B. The expressions listed there were used to develop a Matlab program that shows the transmission's dependence on the wavelength, in the beam splitter. When optimizing the transmission for $\lambda = 800$ nm for both polarizations, the results in Figure 3.6 were obtained.

The parameters were set to:

$n_1 = n_3 = 1{,}46$ (fused silica)
$n_2 = 1$ (air)
$\theta_{in} = 45°$

Note that the distance d between the prisms is adapted to the polarization, that is: $d_s = 224{,}58$ nm and $d_p = 374{,}15$ nm. S stands for perpendicular polarization and p for parallel polarization.

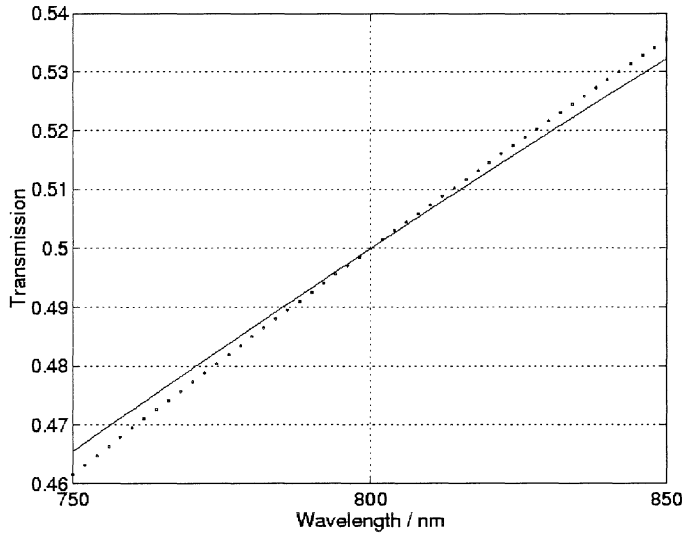

Figure 3.6 The transmission as a function of wavelength, for s-polarized (solid line) and p-polarized (dotted line) light, in a FTIR beam splitter.

Clearly, the s-polarized light responds to our demand better than the p-polarized light, so from now on the focus is on this polarization.

To estimate the part of the ASE leaving the interferometer, it is now possible to form

$$(\Im - \Re)^2 = (2\Im - 1)^2$$

It is further assumed that the spectral shape of the beam entering the interferometer is Gaussian, with its peak at $\lambda = 800$ nm and with a bandwidth, $\Delta\lambda$, at FWHM of 60 nm:

$$I = I_0 e^{-\frac{2(\omega-\omega_0)^2}{\sigma^2}} \tag{3.18}$$

where $\sigma = \frac{\pi c \Delta\lambda}{\lambda^2}$ and $\omega = \frac{2\pi c}{\lambda}$

The beam at the output of the linear Sagnac interferometer is calculated by the integral:

$$I_B = \int_{-\infty}^{+\infty} (2\Im(\omega) - 1)^2 I(\omega) d\omega \tag{3.19}$$

A comparison between I and I_B could now be made, (Figure 3.7). The drop of intensity at 800 nm corresponds to a reflectivity of 50 %.

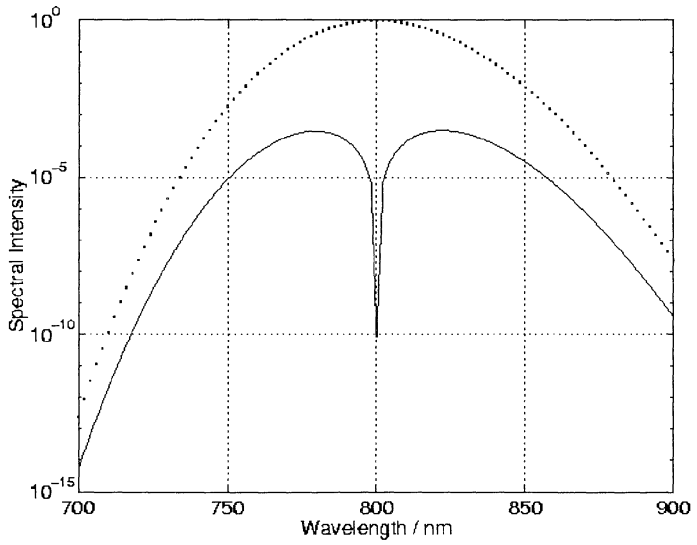

Figure 3.7 Spectral intensity at the input of the interferometer (dotted line) and at the output (solid line) with a beam splitter based on FTIR.

The numeric value of the integral (3.19) is $3{,}8 \times 10^{-4}$ for the s-polarization. The same calculation for the p-polarization gives the value $4{,}7 \times 10^{-4}$ which is less optimal than for the s-polarized light, just as expected.

With a beam splitter with no losses assumed and the distance between the prisms optimized, there would thus be an improvement of the contrast with less than a factor 10^4. It is too far from our objective to be satisfying, and a better solution had to be found.

3.4.2 Beam Splitter from Melles Griot

To obtain a more significant improvement of the contrast than with the previously described beam splitter, it was obviously necessary to approach the condition $\Re = \Im = 1/2$ over a wider spectral range. We requested specifications from the manufacturer Melles Griot of the beam splitter on the market that best served our purposes (supplement 1), and calculations, similar to those for the FTIR beam splitter, were performed.

For an angle of incidence of 45° with s-polarized light, it showed a promising shape of the transmission versus the wavelength, see Figure 3.8. A polynomial fit for the given data was made to obtain the curve.

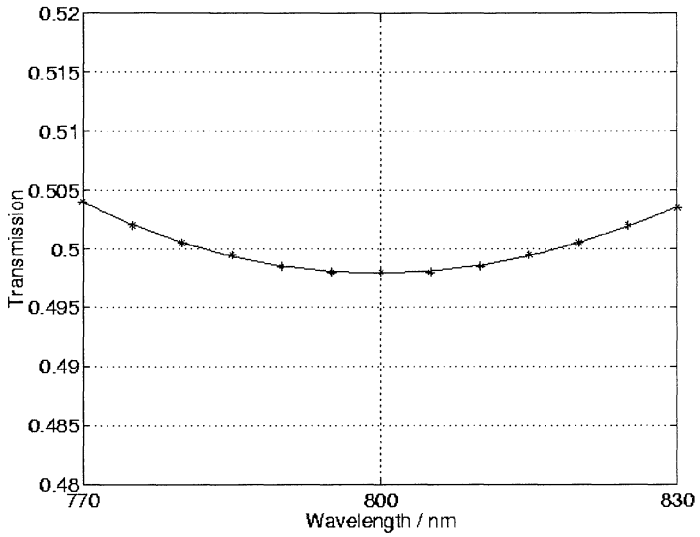

Figure 3.8 The transmission as a function of wavelength for a Melles Griot beam splitter. The spots are taken from the received data, and the curve is a polynomial fit to these.

By describing the transmission over the spectral range of interest with the same polynomial, simulations similar to those made for the FTIR beam splitter could be accomplished. The same Gaussian beam was assumed to enter the interferometer, and the beam at the output was calculated, see Figure 3.9. The two drops of intensity correspond to the wavelengths in Figure 3.8 where the reflectivity equals 50 %.

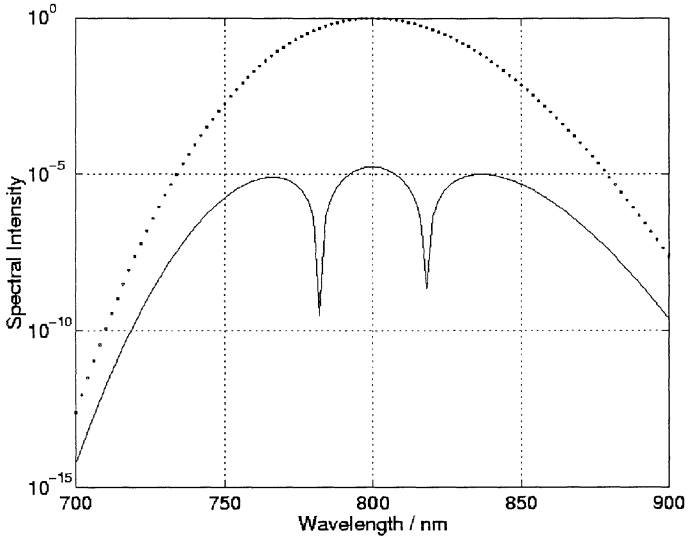

Figure 3.9 Spectral intensity at the input of the interferometer (dotted line) and at the output (solid line) with a Melles Griot beam splitter.

Calculating the integral (3.19) gives the numeric value $1{,}9 \times 10^{-5}$, which is almost a factor ten better than for the FTIR beam splitter. It is fairly close to our objective, and the Melles Griot beam splitter was thus selected for the experiments.

3.5 Spatial Effects

In order to investigate the effect of the non-linear Sagnac interferometer on the spatial distribution of the beam, a program was written in Matlab to simulate different possible scenarios. The simulations were based on Equation (3.17). Further it was assumed that $\Re = \Im = ½$ which gives the transmission of the Sagnac interferometer $\Im = \frac{1}{2}(1-\cos\Delta\varphi)$ if no neutral density is inserted in the beam path. The following assumptions were used throughout the simulations:

$n_2 = 3{,}2\times10^{-16}$ cm²/W (fused silica)
$\lambda = 800$ nm
$L = L_1 + L_2 = 1$ cm
$w = 5$ mm (see Appendix A)

The neutral density τ was set to zero, while the phase shift was calculated. Yet, the beam was assumed to pass through the interferometer without obstacles. We approximated the beam entering the interferometer as Gaussian, $I = I_0 e^{-2\frac{r^2}{\omega^2}}$, and obtained the results in Figure 3.10 and 3.11 below.

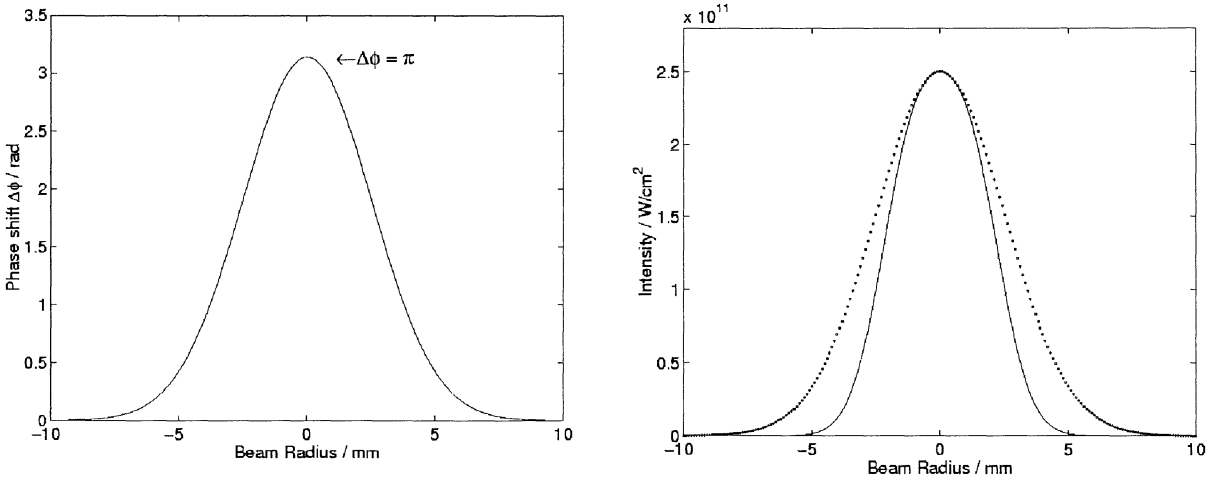

(a) (b)

Figure 3.10 Phase shift (a) and spatial distribution (b) at the input (dotted line) and output (solid line) of the interferometer, for a Gaussian beam with $I_0 = \lambda / n_2$

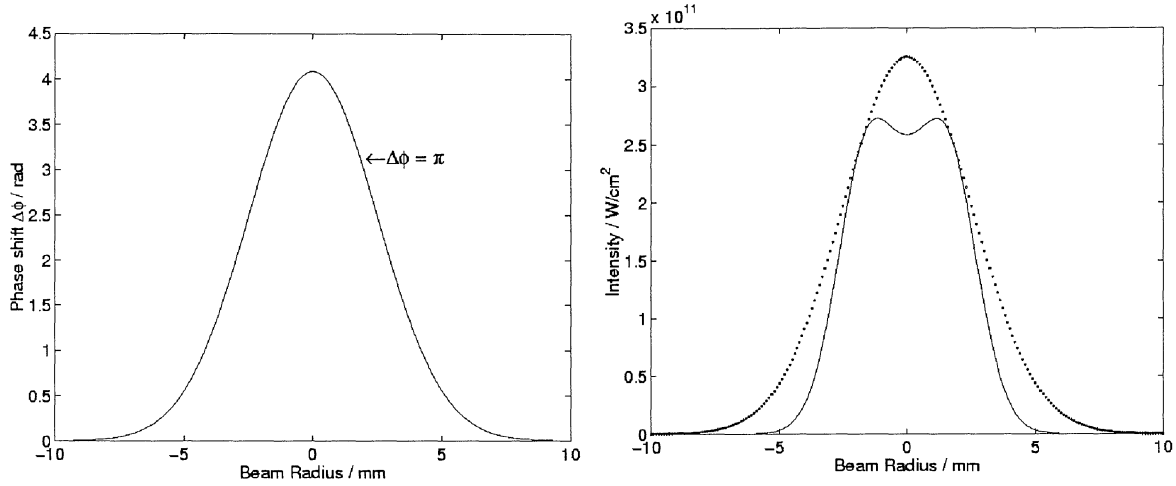

(a) (b)

Figure 3.11 Phase shift (a) and spatial distribution (b) at the input (dotted line) and output (solid line) of the interferometer, for a Gaussian beam with $I_0 = 1{,}3 \times \lambda / n_2$

Note that while arranging the interferometer in order to obtain a phase shift of π below the peak of the beam, the beam shape is modified in the middle. Normally, this will cause no problem, since the modification will be compensated for in the following amplification process.

As a matter of fact, the laser beam used in the experiments was not a true Gaussian, but rather a super Gaussian beam of the form $I = I_0 e^{-2\frac{r^4}{\omega^4}}$. A simulation with this beam was thus of considerable interest, see Figure 3.12.

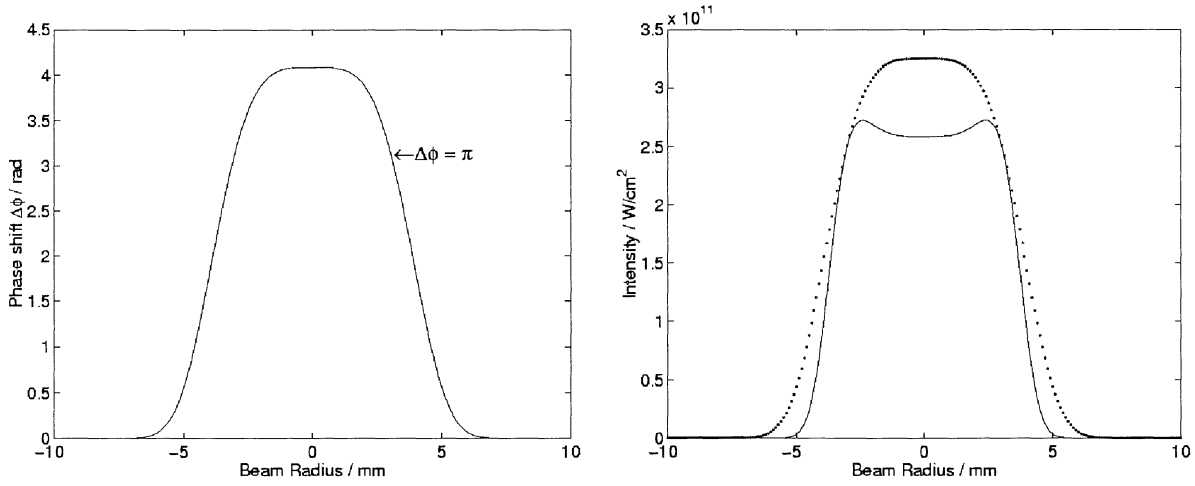

(a) (b)

Figure 3.12 Phase shift (a) and spatial distribution (b) at the input (dotted line) and output (solid line) of the interferometer, for a super Gaussian beam with $I_0 = 1{,}3 \times \lambda / n_2$

The modification of the beam shape is less significant for the super Gaussian beam, which means that the following amplification process will compensate even better for it.

4 Experiments with a Continuous-Wave Laser

A continuous-wave laser with low energy was used to investigate the behavior of the linear Sagnac interferometer. The measured reduction of the intensity of this laser beam could indicate what to expect from the ASE in coming experiments, with a high power laser.

4.1 Experimental Setup

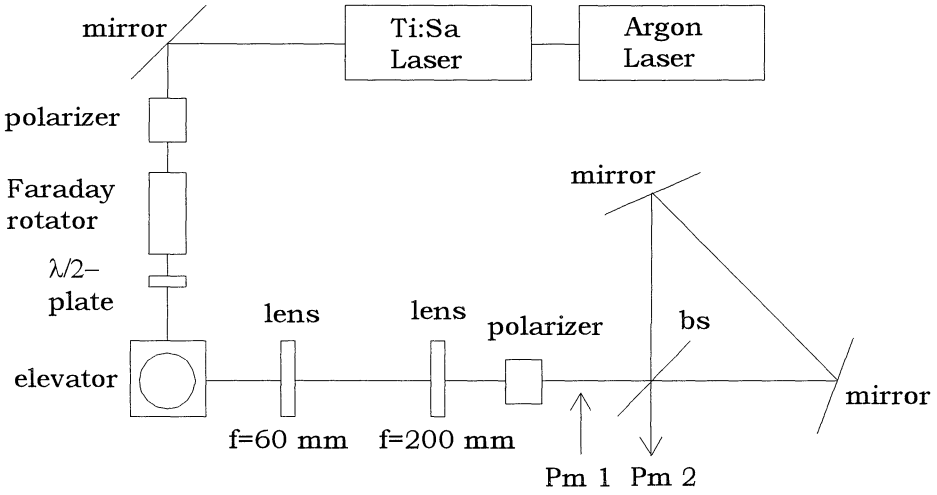

Figure 4.1 Schematic view of the experimental setup. Pm stands for power meter and bs for beam splitter.

An argon laser was used to pump a titanium doped sapphire crystal, sending out light at a wavelength of approximately 800 nm. The maximum output power of the laser was 1,5 W. In our experiments we confined ourselves to a maximum output of about 300 mW.

Firstly, the beam was oriented towards an elevator, consisting of two mirrors. The purpose of the elevator was to raise the beam to the level of the interferometer, and to change the p-polarization of the laser beam into s-polarization. To obtain the future experimental conditions a telescope was mounted next. The Sagnac interferometer was then put in place. As the beam splitter was optimized for s-polarized light, a polarizer was inserted right in front of it, to ensure an optimal polarization. In order to prevent the reflected beam to reenter the laser, an isolator was finally put in place. The isolator consisted of a Faraday rotator that rotates the beam 45°, followed by a half wave plate that rotates it back 45°. Consequently, the beam heading towards the interferometer does not experience any shift in polarization. However, the reflected beam does, because in this direction the half wave plate and the Faraday rotator do not cancel each other, but add. The s-polarized light propagating back towards the laser comes out from the elevator p-polarized [12]. As the polarizer behind lets no such light through, the reflection is stopped.

Comparisons were made between the maximum output power and the input power, and as they came out almost identical (an error of less than 4 %), for simplicity the measurements were performed with the power meters 1 and 2 in Figure 4.1. The output power divided by the input power gave the degree of extinction of the beam. Losses in the beam splitter and in the mirrors were thus neglected.

4.2 Results

As the beam splitter was optimized for s-polarized light, an incident angle of 45° and certain wavelengths (see supplement 2), these were the parameters chosen to extinguish the beam at the output of the interferometer. The output power of the laser had to be considered, as it was a function of the wavelength. For an incident angle of 45° and the optimal polarization, the results in Figure 4.2 were obtained. The wavelength was varied in steps of 10 nm, and the output and input powers were measured.

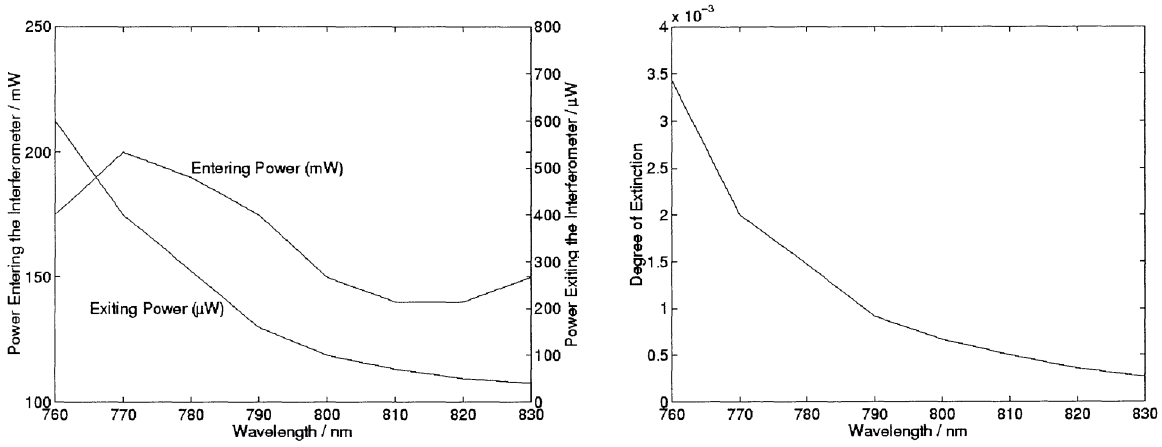

(a) (b)

Figure 4.2 In (a) the power entering and exiting the interferometer, and in (b) the degree of extinction, at an incident angle of 45°.

The extinction was good at long wavelengths, but the curve was not flat enough. By changing the incident angle to 44°, a better extinction was reached, see Figure 4.3.

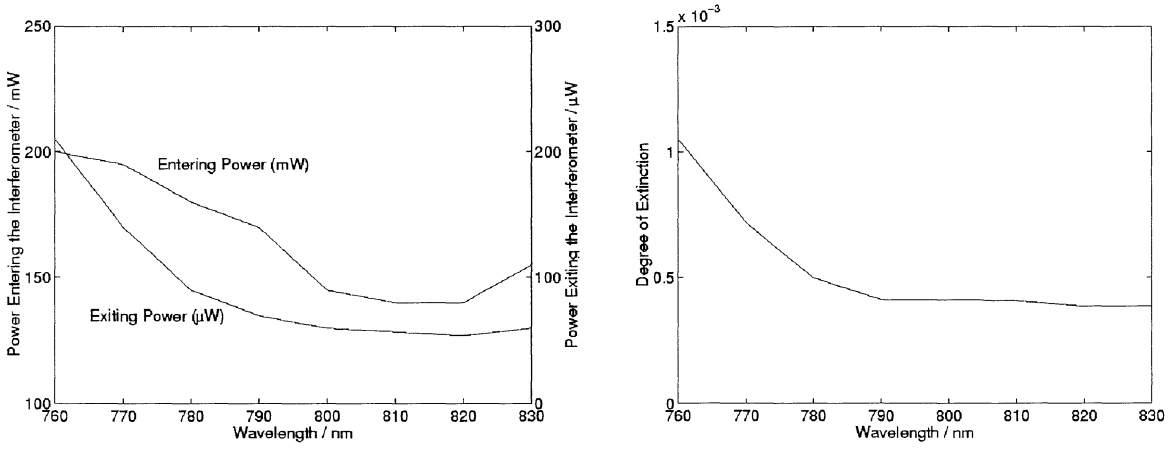

(a) (b)

Figure 4.3 In (a) the power entering and exiting the interferometer, and in (b) the degree of extinction, at an incident angle of 44°.

Figure 4.3.b shows a very promising result, since the extinction curve is flat on a high degree of extinction. The flatness of the extinction curve indicates that the beam splitter is well optimized over a wide spectral range. Since the ASE coming from the femtosecond chain has a bandwidth of approximately 30 nm, it seems feasible to obtain a uniform extinction over the whole beam.

These results were achieved as the short arms of the interferometer were about 30 centimeters long. It was suggested that a shortening of these, to 15 centimeters, would improve the extinction. The only thing gained was, however, a somewhat better stability of the interference.

When a non-linear element was introduced into the beam path inside the interferometer, the high extinction was lost. Obviously, the optical quality of the components is of great importance. As a consequence the used mirrors were changed for others with higher optical quality, which improved the results with a factor 2, to $0{,}2\times10^{-3}$. This indicates that, when applied to a femtosecond laser, this interferometer would improve the contrast with a factor 5 000, which would be a highly satisfying result.

One major problem with this interferometer is that part of the incident beam is reflected in the anti reflection coated surface, which in fact reflects about one percent of the beam. A second, lower intensity, beam arises parallelly to the main one. Between the main and the secondary beam there is a phase shift of π, because the beam reflected in the anti reflection coated surface is twice reflected towards a lower index medium, instead of once. The consequence is that when the main beam is extinguished, the secondary is at its maximum. The above measured powers include both beams.

Attempts were made to remove the disturbing reflection at the output, and it seemed to improve the results considerably, with at least a factor two. The difficulty was to completely let through the beam of interest while the second was totally stopped. As the beam splitter is fairly thin (a few millimeters) the two exiting beams are hardly separable.

5 Experiments with a Femtosecond Pulsed Laser

5.1 Experimental Setup

The Sagnac interferometer was put in Salle Turquoise, at LOA, to perform experiments with an ultra short-pulse intense laser beam. A general overview of the laser in this room is shown in Figure 5.1. The Pockels cell sets the repetition rate to 1 kHz. The energy at the output is about 1 mJ and the time duration of the pulse is in the order of 50 fs. For more information about this laser chain, consult [13].

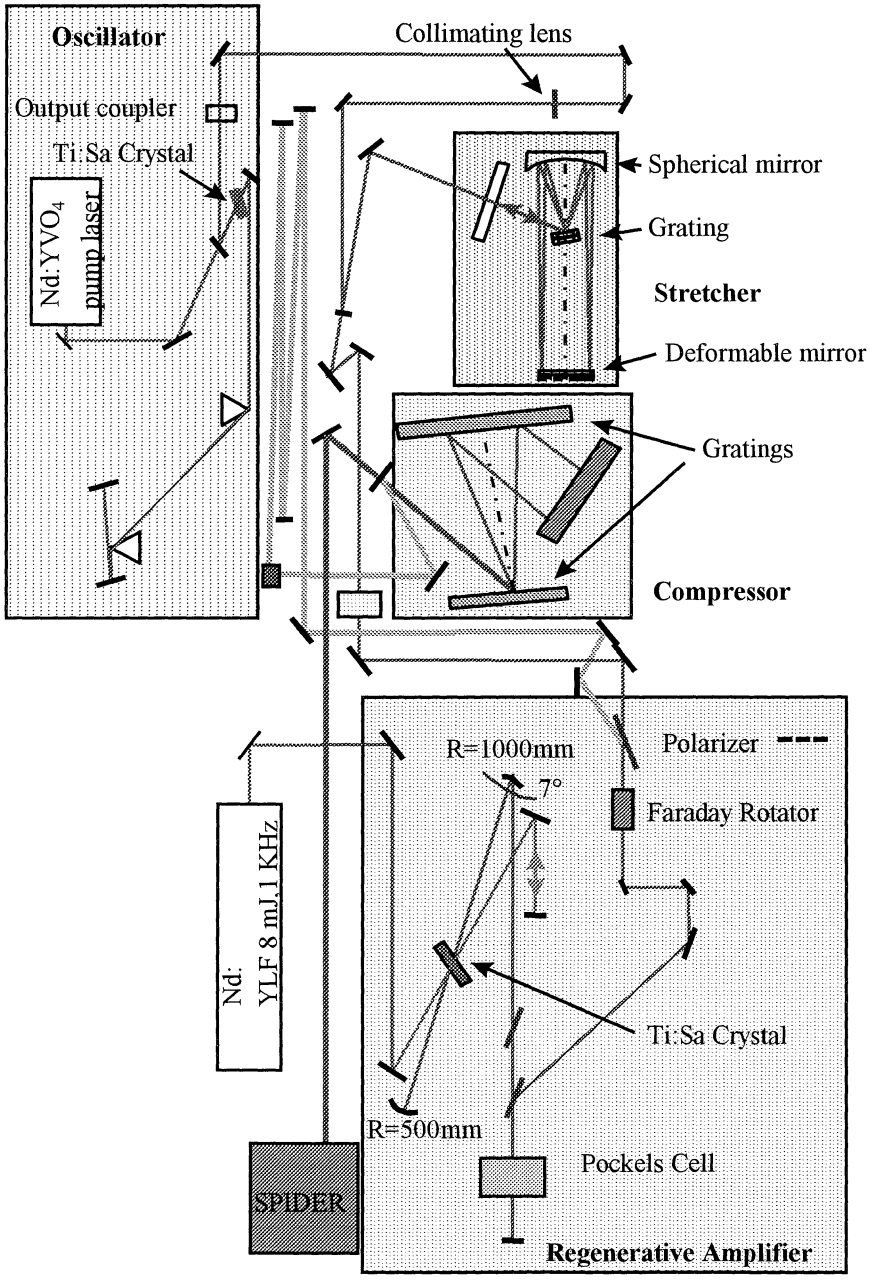

Figure 5.1 Overview of the laser chain in Salle Turquoise at LOA in Paris.

At the output of the laser chain, the Sagnac interferometer was mounted along with other optical components, see Figure 5.2.

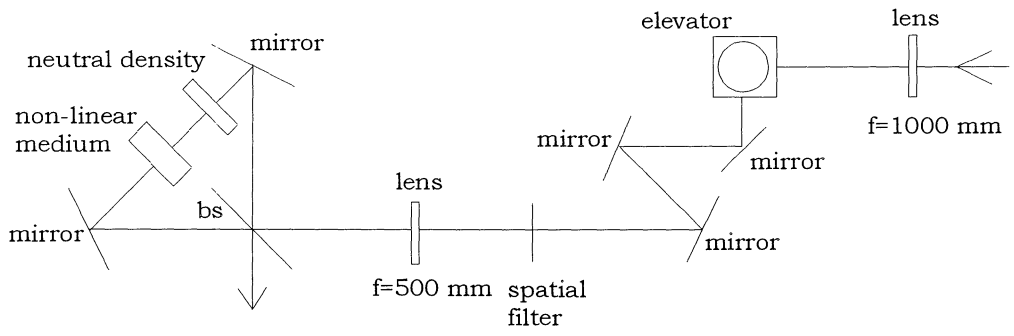

Figure 5.2 Schematic view of the experimental setup.

The lenses reduce the size of the beam, and the elevator changes its polarization, to s-polarization. The spatial filter was put in the Fourier plane of the lens with a focal length of 500 mm, to remove disturbing spatial frequencies and get a cleaner mode.

5.2 Results

5.2.1 Experiments with Fluorescence in a Linear Sagnac Interferometer

First, measurements of the degree of extinction of the fluorescence, coming from the regenerative amplifier, were performed. There was thus no pulse at this moment. The fluorescence corresponds to the ASE in the ultra short pulse. During these experiments, no non-linear element or neutral density was inserted in the interferometer. A polarizer was on the other hand inserted at the output of the laser, to ensure optimal polarization.

The incident angle was changed, in steps of one degree, and the input and output power of the interferometer were measured. As mentioned in chapter 4.2, two beams that are out of phase with each other with a factor π are exiting the interferometer. It is impossible to entirely separate them, but with a pinhole at the output, a fairly good screening of the secondary beam was obtained. To get an idea of the results' dependence of whether the secondary beam is screened off or not, measures were performed both with and without this beam. As can be observed in Figure 5.3 a, the output power is considerably lower if only the main beam is regarded. Figure 5.3 b shows the degree of extinction for the main beam.

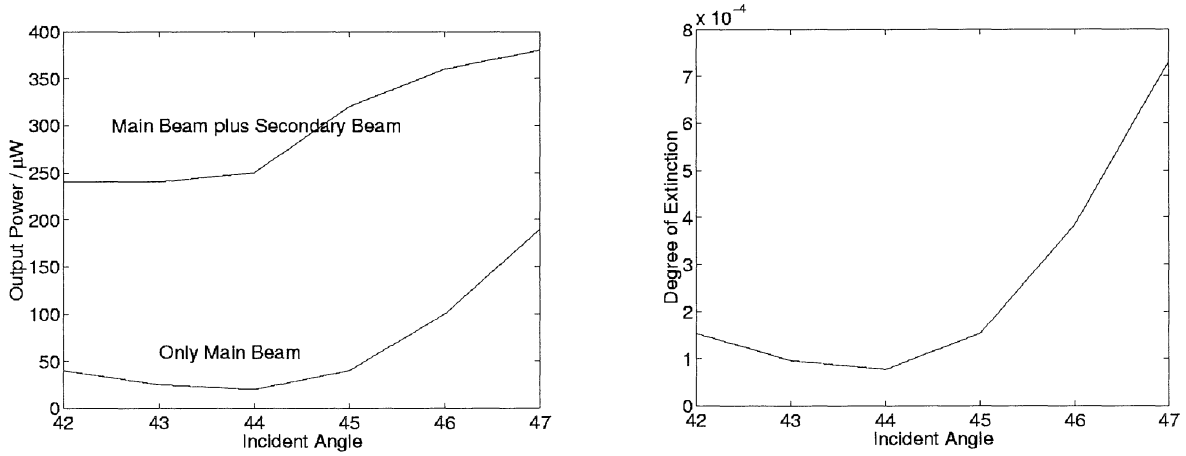

(a) (b)

Figure 5.3 In (a) the output power as a function of the incident angle, measured both with and without screening of the secondary pulse. In (b) the degree of extinction for the main pulse.

Clearly, the optimal incident angle lies around 44°, and the following measurements were performed at this angle. An improvement of the contrast with a factor 10 000 should be attainable with this setup. This is remarkably close to the theoretical optimal result.

To investigate the quality of the beam splitter, the spectra at the output and input of the interferometer were compared, see Figure 5.4. As they come out almost identical, the beam splitter is visibly of satisfying quality. Note that this figure does not allow comparisons of intensity, only of spectral shape. The reason why the drops of intensity in Figure 3.9 do not appear, is probably because the beam splitter nowhere has a reflectivity of exactly fifty percent.

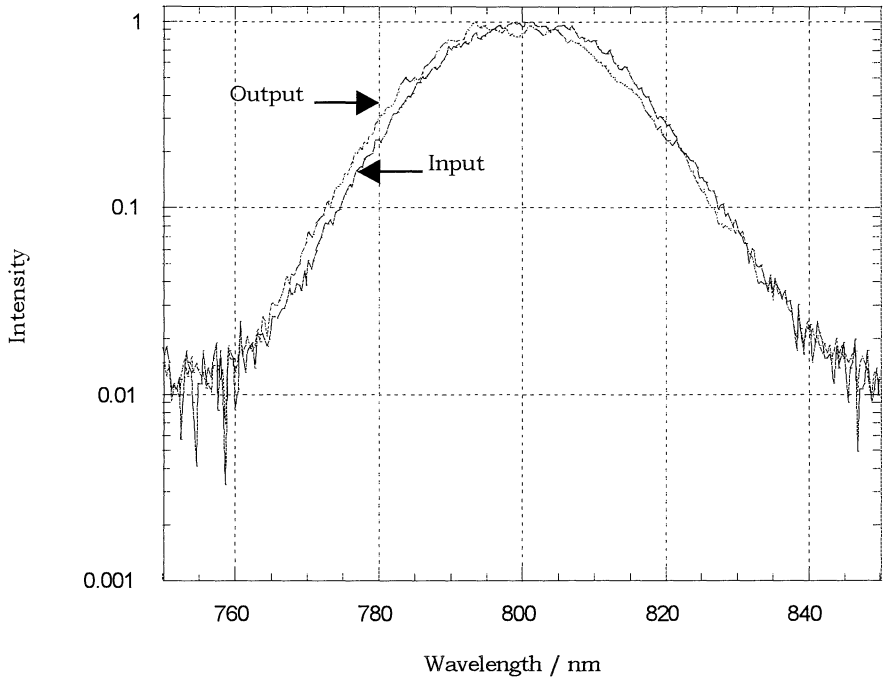

Figure 5.4 Spectral shape of the pulse at the input and at the output of the interferometer.

The fact that the spectral shape of the fluorescence is preserved during passage through the interferometer is very reassuring. The figure shows clearly that the beam splitter responds to different wavelengths in the same way. This result is important, since a modification of the spectral shape of the pulse would have made it impossible to compare coming results with former simulations.

5.2.2 Experiments with a Femtosecond Pulsed Laser in a Non-Linear Sagnac Interferometer

A non-linear element, consisting of fused silica, and a neutral density were placed in the beam path in the interferometer, and the pulsed laser beam was let through. At the adjustment for optimal extinction of the fluorescence, there was however not much intensity at the output of the interferometer, contrary to what was expected. Instead, the main part of the pulsed beam was reflected back towards the laser. An additional non-linear element was inserted to increase the phase shift between the beams. This measure turned out to be insufficient, and in addition stronger densities were tried to increase the phase shift. The output power was measured for a few densities with different optical density inserted in the beam path, see Figure 5.5. The percentage of the maximum output power was also calculated, since the output power decreases for higher optical density.

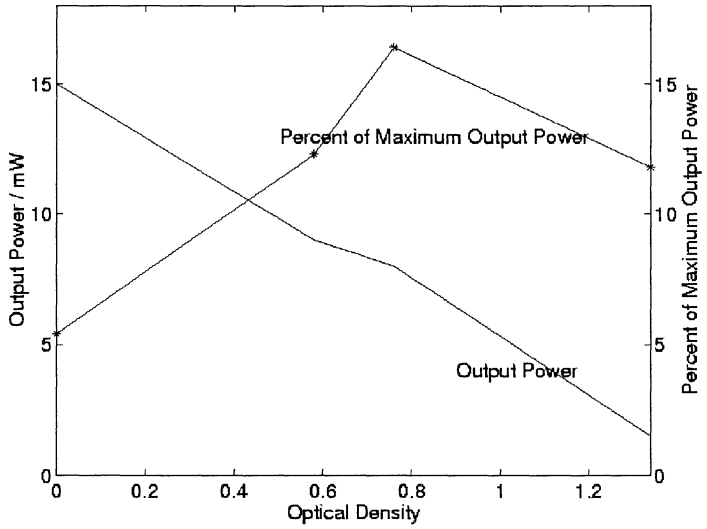

Figure 5.5 Output power and percent of maximal possible output power, as a function of the optical density of the neutral density. The input power was 280 mW.

It is clear that the phase shift is far from π, since even for the best result obtained (optical density = 0,76) only a fraction of the possible output is measured. A phase shift close to π would have given a percentage close to hundred.

It seemed interesting to examine the output power's dependence of the phase shift. A simulation in Matlab, based on equation (3.16), was performed. The optical density was set to 0,76, see Figure 5.6.

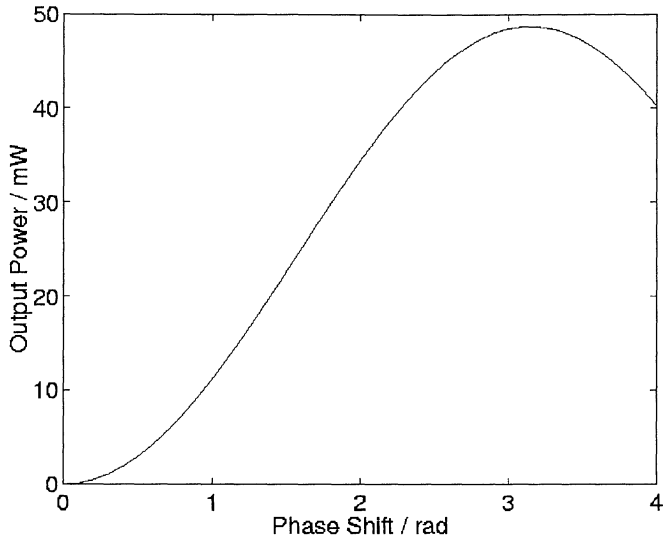

Figure 5.6 The output power as a function of the phase shift, with a neutral density with optical density 0,76 inserted in the interferometer.

Under the same conditions as in the simulation, an output power of 8 mW was measured. According to Figure 5.6 the phase shift is thus less than a third of π, and it is not surprising that the output power is low. As the pulse gets a phase shift different from π it will be partly reflected by the interferometer towards the laser.

According to Figure 5.6, the results should have been better with a stronger neutral density but Figure 5.5 surprisingly contradicts this. The reason could be that the maximum optical density in Figure 5.5 was achieved by putting two neutral densities in the beam path. Previous experiments (chapter 4) have shown that the results are most dependent on the optical quality of the components in the beam path. An additional neutral density has presumably damaged the beam enough to give misleading results.

5.3 Conclusion

The current difficulties associated with the non-linear Sagnac interferometer are the following:

- Difficulty in obtaining a sufficiently high phase shift.
- Strong fluctuations at the output of the interferometer, making measurements unreliable.
- A secondary beam exits the interferometer inconveniently close to the main beam, rendering the measurements even more uncertain.

In order to increase the phase shift, either the beam has to pass through a longer distance of non-linear medium, or a higher intensity, obtained by shortening the time duration of the pulse, is required. A third possibility would be to use a stronger neutral density, but the reduction of the intensity transmitted through the interferometer makes it uninteresting for future applications.

When reducing the time duration of the pulse, non-linear effects were observed in the beam splitter and in the spatial filter. No exact measurements of the time duration were performed, but it was verified that the laser worked close to the shortest obtainable pulse duration, i.e. approximately 50 fs.

To create the phase shift, the optimal solution would be to use a much thicker beam splitter, and no additional non-linear medium. A filter, deposited onto its reflecting surface, would optimize the setup even more. Without the non-linear element and the neutral density in the beam path, better results would certainly be achieved. A thicker beam splitter would also separate the main beam from the secondary one, improving the reliability of the measurements.

In addition, the beam splitter should be larger, to avoid cutting the beam when reflected in it. The beam splitter used in the experiments had a diameter of about 20 mm, and at angles out of 45° it was almost impossible not to cut the beam. This might be a reason to the strong fluctuations at the output of the interferometer, since the beams were perhaps not optimally superposed.

6 Summary and Outlook

In this master thesis a new method to improve the temporal contrast of an ultra short intense pulse has been developed, at the Laboratoire d'Optique Appliquée, in Paris. The technique, using a Sagnac interferometer in combination with non-linear optics, was implemented at a 1 kHz, 50 fs laser at LOA.

The theoretical results were satisfying, showing a possible improvement of the contrast of more than four orders of magnitude. Experiments with a Sagnac interferometer implemented on a continuous-wave laser showed an extinction of low intensity light of up to four orders of magnitude, in accordance with the theory. An extinction of the fluorescence from a 1 kHz, 50 fs laser, of four orders of magnitude was obtained. Experiments with high intense femtosecond pulses were also performed. The setup is at present being worked on at LOA to develop the method further.

The work realized has been accepted for oral presentation at the international Conference on Laser and Electro-Optics (CLEO) and is currently in the process of submission to a scientific journal.

There are other ways proposed to increase the temporal contrast of short intense pulses. One is another non-linear method, using a saturable absorber. It has been implemented and shown an improvement of the contrast of two orders of magnitude [10]. In order to obtain a temporal contrast of up to ten orders of magnitude, the next step would be to combine the non-linear Sagnac interferometer with a saturable absorber in a laser chain. Experiments that need this temporal contrast will then be made possible, opening up new domains of research.

Acknowledgements

First of all I would like to acknowledge my supervisor at LOA, Dr. Gilles Chériaux, for guiding me during this thesis work, and patiently answering all my questions in comprehensive French.

Further I would like to thank:

- My supervisor at LTH in Lund, Professor Anne l'Huillier, for giving me the chance to perform my thesis at LOA, and for encouraging me all the way.
- The director of LOA, Mme Danièle Hulin, for gently receiving me and giving me the opportunity to work under excellent conditions in the laboratories at LOA.
- Mr Jean-Paul Chambaret, for his optimistic enthusiasm for my subject, and his support during my work at LOA.
- Mr Pascal d'Oliveira, for helping me progress in the laboratory and for answering many questions.
- All members of the group ELF and everybody else at LOA, who made it worth taking the RER every morning, to come out to LOA and work with you.
- Frederick Weihe, who corrected my English, and helped me to find the appropriate words where I failed.
- A special thanks to Mlle Octavie Naudet, who with her cheerful temperament and gentle manners embellished my stay in France in several ways. Her hospitality and generosity were greatly appreciated, as were the girl-to-girl chats at work!

Last but not least I want to thank my lovely boyfriend Gustav, who certainly was the greatest support of all. Thanks to him I spent some unforgettable months in the wonderful city of Paris.

References

[1] A. E. Siegman. *Lasers.* University Science Books, 1986.

[2] J. P. Gordon, H. J. Zeiger, C. H. Townes. Physical Review, vol 95, p 282, 1954.

[3] T. H. Maiman. Nature, vol 187, p 493-494, 1960.

[4] Fork, Brito Cruz, Becker, Shank. Optics Letters, vol 12, No 7, p 483, 1987.

[5] D. H. Sutter, G. Steinmeyer, L. Gallmann, N. Matuschek, F. Morier-Genoud, U. Keller. *Semiconductor saturable-absorber mirror-assisted Kerr-lens mode-locked Ti:sapphire laser producing pulses in the two-cycle regime.* Optics Letters, vol 24, No 9, May, 1999.

[6] Mourou, Barty, Perry. *Ultrahigh-Intensity Lasers: Physics of the Extreme on a Tabletop.* Physics Today, p 22, jan 1998.

[7] French. *The Generation of Ultrashort Laser Pulses.* Reports on progress in physics, vol 58, No 2, p 169, feb 1995.

[8] D. Strickland, G. Mourou. *Compression of Amplified Chirped Optical Pulses.* Optics Communications, vol 56, p 219, 1985.

[9] J.D. Bonlie, F. Patterson, D. Price, B. White, P. Springer. *Production of $>10^{21}$ W/cm^2 From a Large-Aperture Ti:sapphire Laser System.* Applied Physics, B 70, p 155-160, 2000.

[10] M. Nantel, J. Itatani, AC Tien, J. Faure, D. Kaplan, M. Bouvier, T. Buma, P. Van Rompay, J. Nees, P. Pronko, D. Umstadter, G. Mourou. *Temporal Contrast in Ti:sapphire Lasers: Characterization and Control.* IEEE Journal of quantum electronics, vol 4, No 2, p 449, 1998.

[11] Dictionary of Scientific Biography, vol XII, p 69, IBN RUSHD, Jean-Servais Stas.

[12] O. Svelto. *Principles of Lasers.* Plenum p 289.

[13] V. Wanman. *Spectral Phase Correction of Femtosecond Pulses Using a Deformable Mirror.* Master Thesis, Lund Reports on Atomic Physics, LRAP-258, Lund, June 2000.

[14] Ian N. Court, Frederick K. von Willisen. *Frustrated Total Internal Reflection and Application of Its Principle to Laser Cavity Design.* Applied Optics, No 6,Vol 3, June 1964.

Appendices

A Gaussian Beams

A Gaussian beam is, slightly simplified, a beam that retains its functional form during propagation through an optical device. This quality makes it advantageous to use Gaussian beams in mathematical simulations, as the formulas become rather simple. Consequently, even when a laser beam is not a true Gaussian, it is common to assume that it is.

The spatial profile of a Gaussian beam, propagating along the z-axis, can be described by the formula:

$$u(x,y,z) = u_0 e^{-\frac{x^2+y^2}{w^2(z)}}$$

where u_0 is the peak amplitude and $w(z)$ is the beam radius at the point where the beam amplitude has decreased with a factor e. The intensity is accordingly given by:

$$I(x,y,z) = I_0 e^{-2\frac{x^2+y^2}{w^2(z)}}$$

where $I_0 = u_0^2$. See Figure A.1.

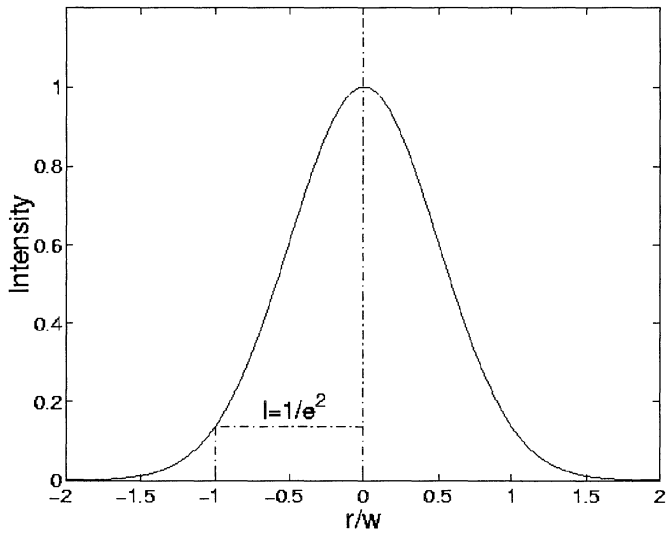

Figure A.1 The spatial profile of a Gaussian beam.

B Frustrated Total Internal Reflection

When a light beam is incident on an interface of two media, part of it is reflected and part of it is transmitted. However, if the index of refraction of the first medium, n_1, is greater than that of the second medium, n_2, and the angle of incidence exceeds the critical angle, θ_c[3] the light will be completely reflected. This is called total internal reflection.

Although the entire beam is reflected, its electromagnetic field will penetrate the second medium a short distance, of the order of the wavelength of the light. The total internal reflection is thus "frustrated". By bringing a third medium close to the first one, this radiation can be coupled into it, and there will be transmission across the boundary. If the second medium has a thickness of the order of the wavelength of the light, a situation like that in Figure B.1 will arise. This phenomenon is also referred to as "optical tunneling", due to its similarity to barrier penetration in quantum mechanics.

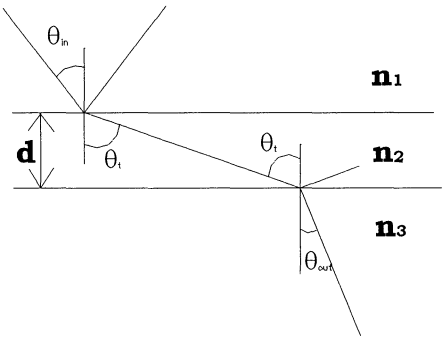

Figure B.1 The effect of frustrated total internal reflection. $\theta_{in} > \theta_c$.

The penetration depth of the electromagnetic field depends on the polarization of the light, so the transmission for both s-and p-polarization, with respect to the plane of incidence, was examined. By using the Fresnel relations the following equations can be derived [14].

$$\Im = \frac{1}{\alpha \sinh^2 y + \beta} \tag{B.1}$$

$$\alpha_s = \frac{(N^2-1)(n^2N^2-1)}{4N^2\cos\theta_{in}(N^2\sin^2\theta_{in}-1)\sqrt{n^2-\sin^2\theta_{in}}} \tag{B.2}$$

$$\alpha_p = \frac{\alpha_s}{n^2}\{(N^2+1)\sin^2\theta_{in}-1\}\{(n^2N^2+1)\sin^2\theta_{in}-n^2\} \tag{B.3}$$

---

[3] $\theta_C = \arcsin(\frac{n_2}{n_1})$

$$\beta_s = \frac{(\sqrt{n^2 - \sin^2\theta_{in}} + \cos\theta_{in})^2}{4\cos\theta_{in}\sqrt{n^2 - \sin^2\theta_{in}}} \tag{B.4}$$

$$\beta_p = \frac{(\sqrt{n^2 - \sin\theta_{in}} + n^2\cos\theta_{in})^2}{4n^2\cos\theta_{in}\sqrt{n^2 - \sin^2\theta_{in}}} \tag{B.5}$$

$$y = 2\pi\frac{n_2 d}{\lambda}\sqrt{N^2\sin^2\theta_{in} - 1} \tag{B.6}$$

where $n = \frac{n_3}{n_1}$ and $N = \frac{n_1}{n_2}$

These expressions can be used to derive the transmission's dependence on the different parameters in a beam splitter based on FTIR.

MELLES GRIOT

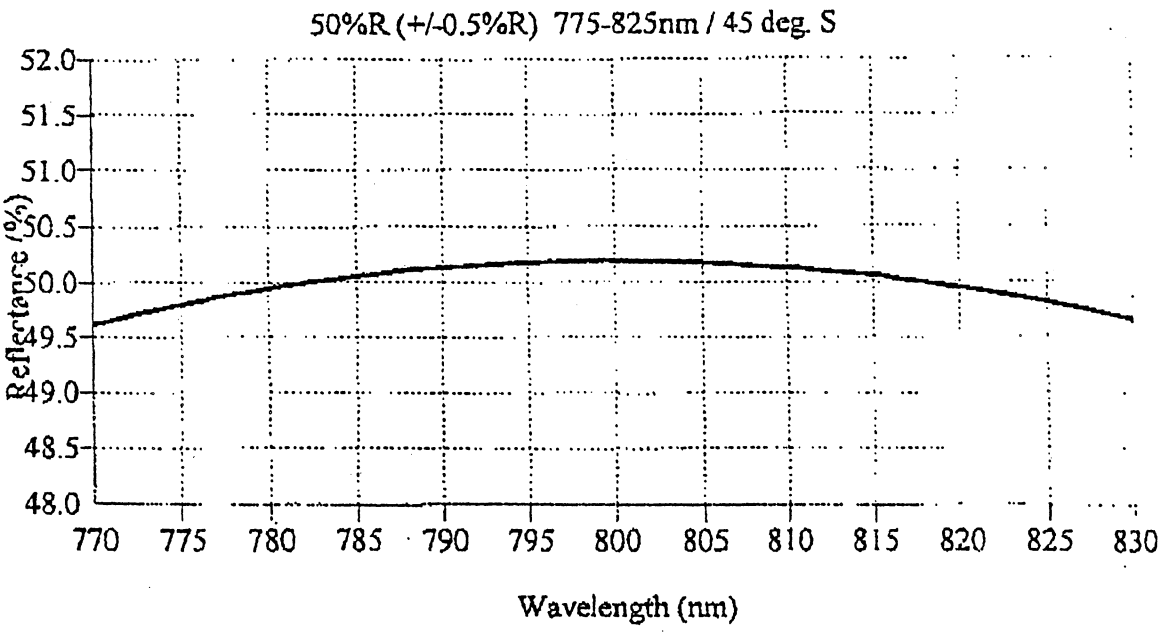

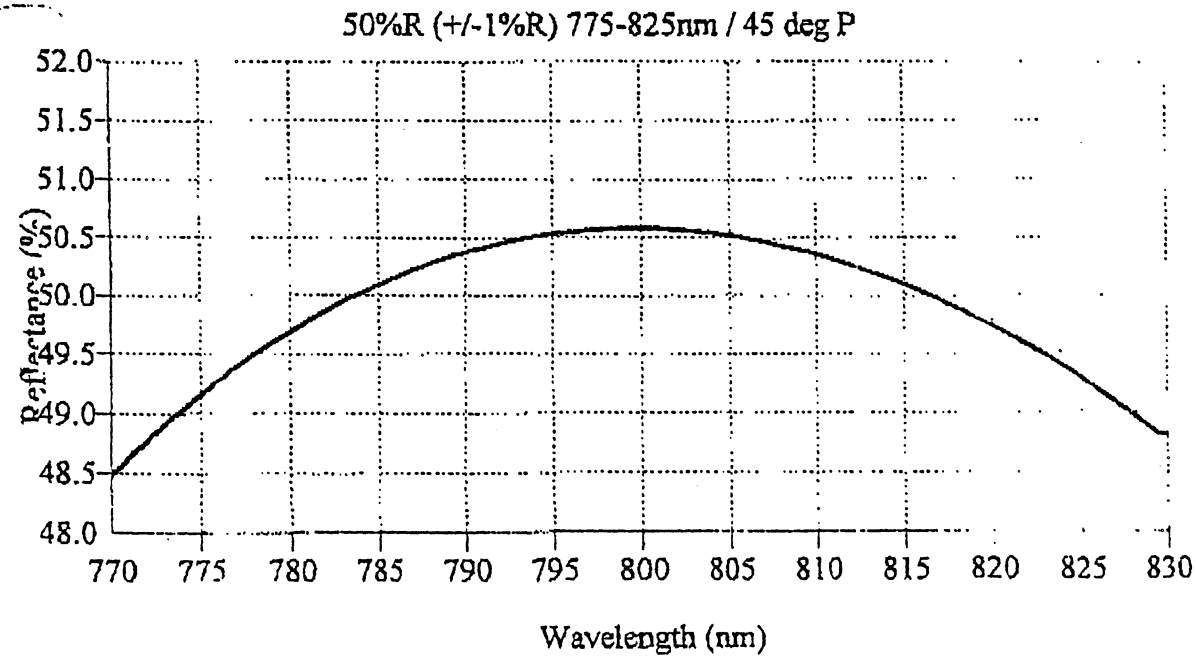

Melles Griot Industrie • FRANCE
12 Avenue Jean BART • 78960 Voisins le Bretonneux • (33)1 30.12.06.80 • FAX (33)1 30.60.08.51

Customer: Melles Griot BV

Order No: 117529

Serial No: 2331 + 2297

Description: 2 off 25mm diameter FS substrates
50%(+/-0.5%)R at 775 – 825nm / 45 deg, s-pol + AR

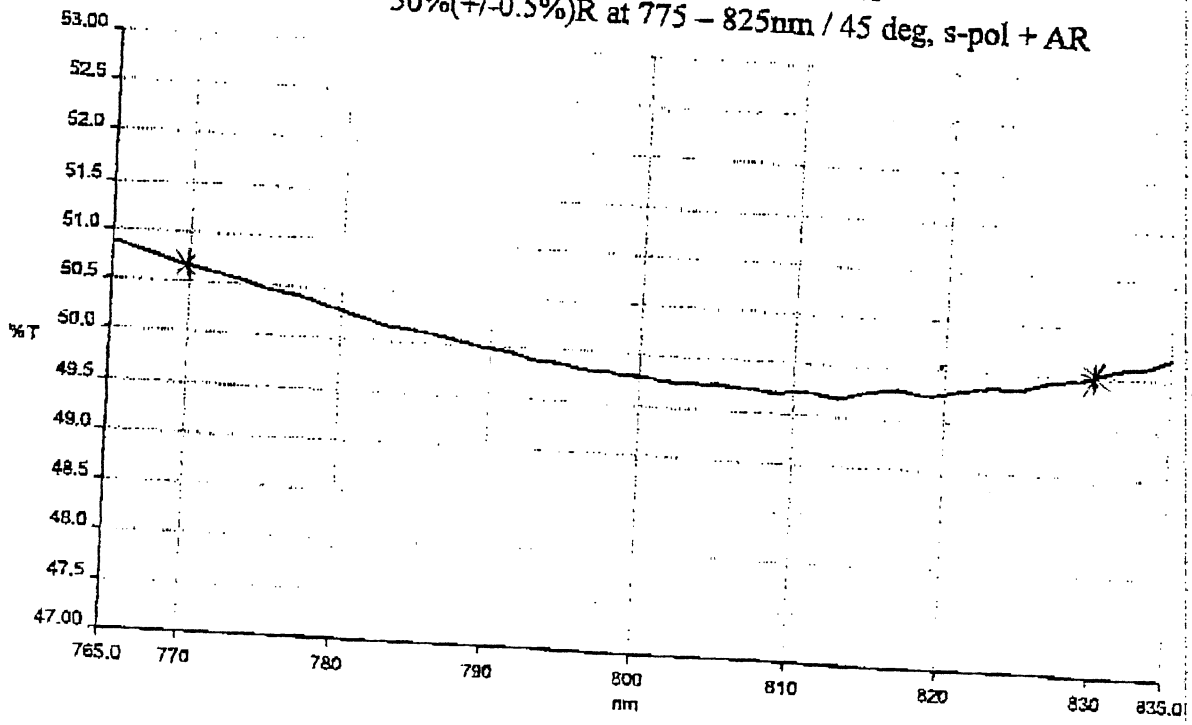

Tested By: RAC

Checked By: Y.B.

Ultrahard coating
This coating meets the following standards with respect to adhesion and resistance to abrasion:
MIL-C-675C, MIL-M-13508C, MIL-C-14806